A neural correlate of visual discomfort from flicker

Carlyn Patterson Gentile

Department of Neurology, Children's Hospital of
Philadelphia, Philadelphia, PA, USA ✉

Geoffrey Karl Aguirre

Department of Neurology, University of Pennsylvania,
Philadelphia, PA, USA ✉

The theory of "visual stress" holds that visual discomfort results from overactivation of the visual cortex. Despite general acceptance, there is a paucity of empirical data that confirm this relationship, particularly for discomfort from visual flicker. We examined the association between neural response and visual discomfort using flickering light of different temporal frequencies that separately targeted the LMS, L-M, and S postreceptoral channels. Given prior work that has shown larger cortical responses to flickering light in people with migraine, we examined 10 headache-free people and 10 migraineurs with visual aura. The stimulus was a uniform field, 50 degrees in diameter, that modulated with high-contrast flicker between 1.625 and 30 Hz. We asked subjects to rate their visual discomfort while we recorded steady-state visually evoked potentials (ssVEPs) from early visual cortex. The peak temporal sensitivity ssVEP amplitude varied by postreceptoral channel and was consistent with the known properties of these visual channels. There was a direct, linear relationship between the amplitude of neural response to a stimulus and the degree of visual discomfort it evoked. No substantive differences between the migraine and control groups were found. These data link increased visual cortical activation with the experience of visual discomfort.

Introduction

Some visual stimuli are uncomfortable to view. High-contrast spatial and temporal patterns (i.e., stripes and flicker) have this property (Wilkins, 1995), particularly when stimulus power is concentrated at frequencies in the midrange of human perception (Fernandez & Wilkins, 2008). Stimuli with these midrange temporal and spatial frequencies generally evoke larger visual cortex responses (Regan, 1983; Tyler, Apkarian, Levi, & Nakayama, 1979) and are detected more easily by human observers when presented at low contrast (Robson, 1966). These findings have led to the general proposal that visually uncomfortable stimuli are the result of "excessive" cortical activity

(Aurora & Wilkinson, 2007). This account finds further support in the observation that people with migraine have both greater discomfort from flickering light (Yoshimoto et al., 2017) and an enhanced visual cortex response to these stimuli (Datta, Aguirre, Hu, Detre, & Cucchiara, 2013; Shibata, Yamane, Nishimura, Kondo, & Otuka, 2011).

Beyond this general proposal, however, the link between specific stimulus properties, visual discomfort, and cortical response is less clear. Only a weak or even absent correlation between visual discomfort and evoked cortical response in people without migraine has been found for stimuli varying in spatial frequency (Huang, Cooper, Satana, Kaufman, & Cao, 2003; O'Hare, 2017). Studies of sensitivity to patterns and temporal flicker have generally been made using black-and-white patterns, which probe only a small set of possible stimulus properties that may be associated with visual discomfort. The cortical visual system receives input via three different postreceptoral channels, each with different spectral (i.e., "color") sensitivity. The LMS ("luminance"), L-M ("red-green"), and S ("blue-yellow") channels also have different spatial and temporal response properties (Kelly, 1974). Prior studies have found a relationship between reported discomfort and the chromatic contrast of spatial gratings (as expressed as distance in hue spaces; Haigh et al., 2013; Juricevic, Land, Wilkins, & Webster, 2010), suggesting that multiple postreceptoral channels contribute to visual discomfort. However, no study has examined the interaction of temporal flicker and postreceptoral channel in the induction of visual discomfort. Recent work has found that pulses of colored light from a dark background differ in the degree to which they evoke discomfort in people who are in the midst of a migraine headache (Noseda et al., 2016, 2017). While again suggesting that the chromatic content of a stimulus influences visual discomfort, studies of this kind are unable to identify the contribution of the different postreceptoral pathways to discomfort. As opposed to a flash of light from darkness, a time-varying modulation of the spectral content of light around a photopic background may be used to selectively target

the postreceptoral visual pathways using the principle of silent substitution (Esteˊvez & Spekreijse, 1982). This approach is well suited to explore the relationship between visual discomfort and visual cortex responses.

Here we examine the association between visual discomfort and evoked response in early visual cortex using flicker of different temporal frequencies that separately target the LMS, L-M, and S postreceptoral pathways. Our goal was to test the hypothesis that greater neural response evoked by any particular stimulus would be associated with a report of greater visual discomfort. We obtained data from 20 subjects: 10 with migraine with visual aura (MwA) and 10 headache-free controls (HAf). We did not observe a difference between the groups in the cortical response to our stimuli, although this comparison was powered to detect only a large effect size. We did, however, find a remarkably close relationship between the tendency of each stimulus to produce visual discomfort and the magnitude of evoked cortical response.

Methods

This study was preregistered on the Open Science Framework (https://osf.io/f7n3x/).

Subjects

Subjects were ages 25 to 41 years and recruited from the greater Philadelphia area and University of Pennsylvania campus, in many cases using advertising on digital social media services. All candidate subjects underwent screening using the Penn Online Evaluation of Migraine (Kaiser, Igdalova, Aguirre, & Cucchiara, 2019), which implements an automated diagnostic survey using the International Classification of Headache Disorders (ICHD)–3 criteria. We identified 10 subjects who met criteria for a diagnosis of MwA. To be included in the study, MwA subjects also needed to report ictal visual discomfort, as determined by a score of 6 or greater on the Choi visual sensitivity scale (Choi et al., 2009), and a response of "yes" to the question in the Choi instrument regarding the presence of light sensitivity during headache-free periods. We also studied 10 control participants who were either entirely headache free or had a history of only mild, nonmigrainous headache. Control subjects were required to have no known family history of migraine and no history of childhood motion sickness. Finally, controls subjects had to score 7 or lower on the Conlon Visual Discomfort Scale (VDS) survey (Conlon, Lovegrove, Chekaluk, & Pattison, 1999). There was no required score for the MwA participants, although we found that these subjects reported higher visual

discomfort as measured by this instrument. Table 1 summarizes the demographic information and survey results for the participants. The study was approved by the Institutional Review Board of the University of Pennsylvania. All subjects provided informed written consent, and all experiments adhered to the tenets of the Declaration of Helsinki.

The demographics of the two groups did not differ significantly by sex ($p = 0.2$), although there were more women than men in the study, consistent with the known demographics of migraine (Goadsby, Lipton, & Ferrari, 2002). The Conlon VDS score was higher in the MwA group ($p = 0.001$). The MwA subjects had a broad range of disease burden, with a median of 11 headache days in the past 3 months (range 0–30 headache days over 3 months), which was significantly higher than the median number of headache days in the headache-free group ($p = 0.0008$). None of the MwA subjects were on preventative migraine medications. One HAf subject reported the use of daily magnesium, and two HAf subjects reported the use of serotonin-reuptake inhibitors, presumably for management of mood.

Candidates were excluded for a history of glaucoma, generalized epilepsy, a concussion in the past 6 months, or ongoing symptoms from head trauma/concussion. Participants were excluded if best-corrected distance acuity was below 20/40 based on the Snellen eye chart or if they did not have normal color vision as judged by the Ishihara test (Clark, 1924).

Visual stimuli and task

Visual stimuli were created using the Metropsis system (Cambridge Research Systems, Rochester, UK). This commercial apparatus for psychophysics implements tests in the Psykinematix language and uses a high-bit depth display with a 120-Hz refresh rate. Photometric calibration of the display was performed with a PR670 spectroradiometer (Photo Research, Topanga Canyon Place, CA). The stimulus was a circular field, 50 degrees of visual angle in diameter, with the outer edge smoothed by a Gaussian envelope (5 degrees standard deviation; Figure 1A). Outside of the stimulus field, the display was set to the half-on primaries.

The spectral content of the stimulus field was modulated in time following a sinusoidal profile to create time-varying contrast that targeted the LMS, L-M, and S pathways (Figure 1B; also see Supplementary Figure S1 for predicted and measured spectra). We used the method of silent substitution to target cone classes alone or in combination. Our estimates of photoreceptor spectral sensitivities were as previously described (Spitschan, Datta, Stern, Brainard, & Aguirre, 2016) and accounted for field size and age (Comission Internationale de L'Eclairage [CIE], 2005).

Variable	MwA (*n* = 10)	HAf (*n* = 10)	*p* value
Age (y)	34 (25–37)	28 (25–41)	0.9
Sex	M 1, F 9	M 4, F 6	0.1
VDS	15 (5–36)	4 (0–6)	0.001
No. of headache days/3 months	11 (0–30)	1 (0–4)	0.0008

Table 1. Subject demographics. *Notes:* The median and range are shown for age, sex, VDS, and number of headache days in the past 3 months. The *p* values represent two-tailed *t* test.
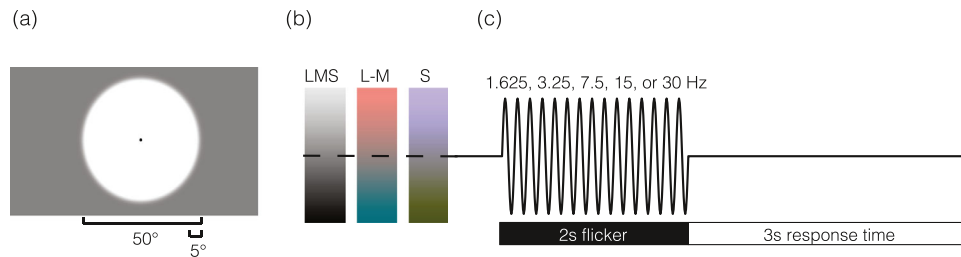

Figure 1. Spatial, temporal, and spectral properties of visual stimuli. (a) The spatial structure of the stimulus consisted of a 50-degree diameter circle, with a 5-degree Gaussian envelope applied to the edge. The entire screen, as well as the stimulus background, was set to a midpoint gray. A 0.2-degree black circle was located in the center of the screen to aid fixation and obscure the foveal blue scotoma (Magnussen, Spillmann, Stürzel, & Werner, 2001). (b) Stimuli consisted of three spectral modulations that targeted the LMS ("black-white"), L-M ("red-green"), and S ("blue-yellow") pathways. (c) Stimuli flickered sinusoidally at a rate of 1.625, 3.25, 7.5, 15, or 30 Hz. Two-second periods of flicker were followed by a 3-s response window during which the midpoint gray screen returned.

The estimates assumed a 32-year-old observer with a 2-mm diameter pupil. Modulation spectra were defined around the half-on (59 cd/m^2) primaries and were designed to produce isolated contrast on the LMS, L-M, and S mechanisms.

Predicted cone spectral sensitivity varies as a function of eccentric field position due to the effect of macular pigment. Failure to account for this effect would produce differential contrast upon the targeted cone mechanism as a function of eccentricity and inadvertent contrast upon nominally silenced mechanisms. To account for this, we varied the chromatic spectral modulations on the screen as a function of eccentricity. Although the CIE standard specifies fundamentals only for field sizes up to 10 degrees, we obtained estimates out to 30 degrees by extrapolation as described previously (Spitschan, Aguirre, & Brainard, 2015). The result was nominal Michelson contrast of 90%, 5.9%, and 81% upon the LMS, L-M, and S channels (respectively) that was spatially uniform across the stimulus field. These contrast levels represent 90% of the maximum possible on the display given its gamut. The 10% "headroom" was reserved to allow for stimulus adjustment by flicker photometry to null residual luminance in the chromatic modulations for each subject. Subjects were shown the 50-degree sinusoidal flickering field that modulated around the background gray at 30 Hz. Subjects were asked to adjust the stimulus field to null residual luminance flicker by pressing the "up" or "down" arrow

on the keypad, which added or subtracted 0.05 from the R, G, and B primary values. This test was repeated twice, once from below the estimated target value and once from above. The value from each test was averaged to determine the nulling correction for the L-M and S channels. There was no difference between nulling values in the MwA and HAf groups (Supplementary Figure S2). One subject (MELA_0201) had difficulty following the nulling procedure. For this subject, the median nulling values across subjects was used instead.

On each of many trials, the half-on background was replaced with the stimulus field, which flickered for 2 s at one of five temporal frequencies (1.625, 3.25, 7.5, 15, and 30 Hz; Figure 1C). Due to a coding error, the two lowest frequencies were 1.625 and 3.25 Hz, instead of the intended values of 1.875 and 3.75 Hz. This error caused the stimuli to deviate slightly from proper log spacing. The period of flicker was followed by a 3-s response window during which the half-on background was again presented. Subjects were asked to rate the visual discomfort produced by the flicker on a 0 to 10 scale, with 0 being not uncomfortable at all, 5 being moderately uncomfortable, and 10 being extremely uncomfortable. The verbal response of the subject was recorded with a microphone and subsequently transcribed by the experimenters. A given block of 35 trials targeted a particular postreceptoral mechanism (LMS, L-M, or S), and the frequency order was pseudorandomized within a block. Each block was

run three times for a total of 21 repeats per stimulus condition.

Following our preregistered protocol, we omit from the primary figures the results for the 15-Hz S stimulus. This stimulus produced an unexpected, spatially structured "brightness" modulation. We attempted to determine the source of this percept but were ultimately unsuccessful. This observation could not be accounted for by luminance artifact from the monitor (Supplementary Figure S3). We consider it possible that the effect arises from the spatial variation that we introduced into the stimulus to account for macular pigment, interacting with longitudinal chromatic aberration (Taveras Cruz, He, & Eskew, 2019). As we were not confident in the properties of this particular stimulus, we elected to collect data for the modulation but not include the data in tests of our hypotheses. The omitted data for the 15-Hz S stimulus are shown in Supplementary Figure S4.

Prior to beginning the experiment, ambient room light was adjusted to achieve a pupil size of ∼2.5 mm. Subjects were positioned in a chinrest 400 mm away from the screen.

Steady-state visually evoked potential recording

Prior work comparing functional MRI (fMRI) and visually evoked potential (VEP) suggests that steady-state visually evoked potentials (ssVEPs) are generated predominantly from early visual cortical areas and area MT (Di Russo et al., 2007). We recorded ssVEPs with a single active electrode over Oz based on the 10–20 international criteria for electroencephalogram (EEG) placement over early visual cortex. A ground and reference electrode were placed on each mastoid. The ssVEP signal was recorded using a biopac (Goleta, CA) ERS100c amplifier with a maximum bandwidth of 1 Hz to 10 kHz at a 2 kHz sampling rate.

Data analysis

Data were analyzed using publicly available (https://github.com/gkaguirrelab/vepMELAanalysis), custom MATLAB software. The signal was subject to a 0.5- to 150-Hz bandpass filter to remove nonphysiologic oscillations and a bandstop filter at 60 Hz to remove electrical line noise. Trials with any time point >0.08 mV or all values <0.02 mV were removed to eliminate noisy trials due to poor electrode placement; this constituted 152 out of a total of 6,300 trials in the study (2.4%). The median response across trials in the time domain provided the cortical VEP. The first 0.5 s of the stimulus presentation were discarded to eliminate the onset response, leaving the remaining 1.5-s epoch.

Because the 1.625-Hz and 3.25-Hz stimuli were not bin centered for the Fourier transform with a 1.5-s response epoch, time windows of 1.231 s and 1.538 s were used, respectively, for the analysis of these stimuli. The signal was converted from the time domain into the frequency domain using a discrete Fourier transform. Responses contained a peak at the fundamental flicker frequency of the visual stimulus, which can be seen in power spectral density (PSD) plots (Supplementary Figure S5). Prominent higher harmonic responses are also evident. Each PSD was fit using a previously described technique (Haller et al., 2018) to estimate and remove the aperiodic (nonoscillatory) component of the ssVEP (Supplementary Figure S5). Consistent with previous reports (Haller et al., 2018), the aperiodic signal was greatest at low frequencies and is well described by 1/frequency function. There were no significant differences in the aperiodic signal between groups or stimulus conditions (Supplementary Figure S6). The aperiodic fit was subtracted from the original signal to obtain the periodic signal (Supplementary Figure S5). Median responses for the fundamental flicker frequency of each stimulus were calculated across groups. A two-sample t test was used for subject demographic comparison. The median responses for each group and spectral direction were fit with a difference-of-exponentials model that describes temporal sensitivity (Hawken, Shapley, & Grosof, 1996). Temporal sensitivity fits were used to calculate the peak frequency and peak amplitude for each curve. Estimates of the variability of these measures in our population were obtained by repeating the fitting over 1,000 bootstrap resamples across subjects (with replacement) and calculating 95% confidence intervals.

In supplemental analyses, we examined the response at the second harmonic frequency. As the 2F harmonic of the 30-Hz stimulus overlaps with powerline noise at 60 Hz, it could not be measured directly. Instead, the amplitude of the harmonic response was estimated. We observed that there was a linear relationship between the frequencies of the 1, 2, 3, and 4 harmonics and the response amplitudes. Thus, the amplitude of response at 30 and 90 Hz was used to estimate the response at 60 Hz in this analysis.

In supplemental analyses, we also tested for the presence of narrowband gamma oscillations. This was done by calculating Thomson's multitaper PSD estimate for each trial and taking the median value across trials.

Results

We collected discomfort ratings and ssVEP data from 20 participants while they viewed high-contrast, uniform, widefield flicker of varying temporal frequency
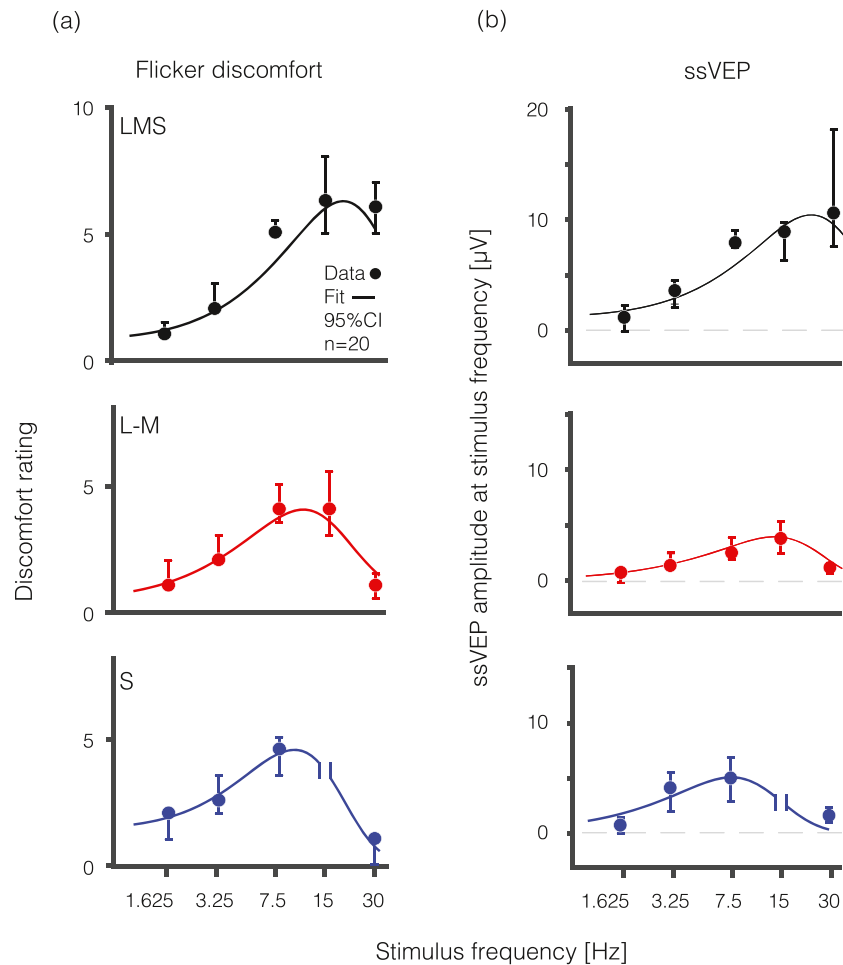
Figure 2. Visual discomfort ratings and visual cortex evoked responses across temporal frequency and spectral modulations. Median visual discomfort ratings on a 0 to 10 scale (a) and visual evoked response at the fundamental stimulus frequency represented in mV (b) are shown as a function of temporal frequency (Hz) for LMS (black), L-M (red), and S (blue) flickering stimuli. Measurements from the S cone directed stimulus flickering at 15 Hz were omitted (following our preregistered protocol) as this stimulus was accompanied by a prominent, spatially structured "brightness" percept that we were unable to remove. Data are collapsed across HAf ($n = 10$) and MwA ($n = 10$) subjects. Error bars represent 95% confidence interval by bootstrap analysis. Fit line is derived from a difference-of-exponentials function.

that targeted the three different postreceptoral pathways (Figure 1). Below, we describe spectral modulations that target the LMS, L-M, or S pathways as having a particular postreceptoral "direction."

We derived the median discomfort rating across participants for each stimulus direction as a function of flicker frequency and derived peak frequency and peak amplitude from fitting a difference-of-exponentials model to the data (Hawken et al., 1996). There were no significant differences between MwA and the headache-free groups for these metrics for any of the postreceptoral directions (Supplementary Table S1). Therefore, we combined the data across the two groups. Supplementary Figure S7 provides the results separated by group.

Discomfort sensitivity to flicker varies by postreceptoral pathway

Visual discomfort ratings varied by flicker frequency and stimulus direction (Figure 2a). Flicker targeting the LMS pathway was found to be most uncomfortable for the highest frequencies presented as compared to stimulation targeting the L-M and S pathways. The estimated temporal peak (and 95% confidence interval) of discomfort sensitivity was 18.6 Hz (16.5–19.4 Hz) for the LMS, 10.3 Hz (9.5–11.6 Hz) for the L-M, and 9.1 Hz (7.8–10.7 Hz) for the S pathway (Table 2). Peak discomfort ratings also varied overall for the different stimulus directions. The greatest degree of discomfort was evoked by flicker directed at the LMS pathway: the

ssVEP	Peak frequency (Hz), median (95% CI)	Peak amplitude (µV), median (95% CI)
Flicker discomfort		
LMS	18.6 (16.5–19.4)	6.3 (5.5–8.0)
L-M	10.3 (9.5–11.6)	4.0 (4.0–5.5)
S	9.1 (7.8–10.7)	4.5 (3.0–5.0)
ssVEP		
LMS	21.8 (17.2–37.9)	10.2 (8.1–17.5)
L-M	13.0 (11.6–15.9)	4.0 (2.7–5.3)
S	7.8 (5.7–9.5)	5.0 (3.5–6.6)

Table 2. Peak frequency and peak amplitude from temporal sensitivity difference of exponentials fit with median value and 95% confidence interval by bootstrap analysis with replacement for the three spectral directions (LMS, L-M, and S).

median (across-subject) peak amplitude of discomfort for the LMS pathway was 6.3 (5.5–8.0) compared to 4.0 (4.0–5.5) for the L-M pathway and 4.5 (3.0–5.0) for the S pathway.

Visual cortex response to flicker varies by postreceptoral pathway

The dependence of the ssVEP upon temporal frequency and stimulus direction was very similar to the relationship seen for visual discomfort (Figure 2b). Flicker directed at the LMS pathway evoked the strongest response for the highest frequencies presented, while peak response occurred at successively lower frequencies for the L-M and S pathways, respectively. The estimated peak of the visual evoked response (and 95% confidence intervals) was 21.8 Hz (17.2–37.9 Hz) for the LMS, 13.0 Hz (11.6–15.9) for the L-M, and 7.8 Hz (5.7–9.5) for the S pathway, all similar to the flicker discomfort data (Table 2). This variation in peak neural response across temporal frequency is similar to what has been observed using fMRI (Spitschan et al., 2016). The amplitude of cortical response also varied for the different stimulus directions. The largest cortical response of 10.2 µV (8.1–17.5) was evoked by flicker targeting the LMS pathway, as compared to 4.0 µV (2.7–5.3) for the L-M pathway and 5.0 µV (3.5–6.6) for the S pathway.

Flicker discomfort strongly correlates with early visual cortex neural response

As the evoked visual cortical response increased, so too did the magnitude of reported discomfort (Figure 3). Neural responses at the fundamental stimulus frequency were highly correlated with the level of reported discomfort from the flicker across the 14 stimulus conditions ($R^2 = 0.83$, $p = 2.2e^{-4}$). This relationship did not appear to be unique to a single postreceptoral channel, and was similar for MwA
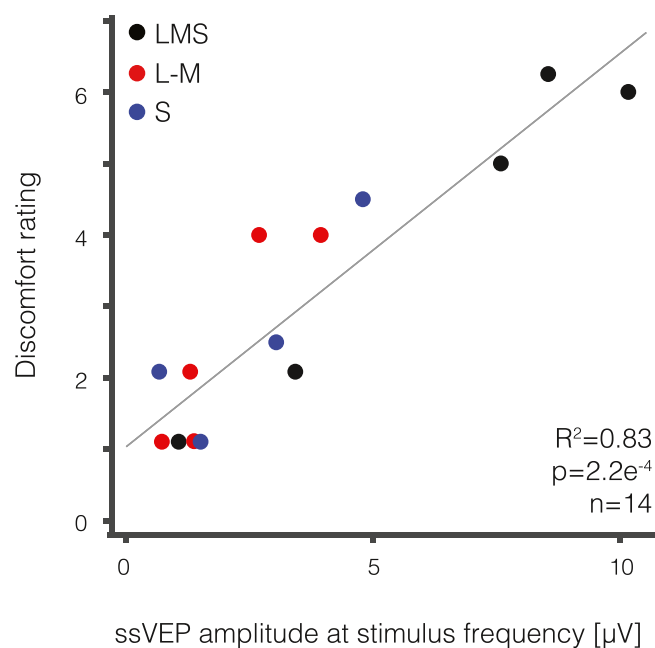

Figure 3. Visual discomfort strongly correlates with visual evoked response. The median visual discomfort rating (0–10 scale) is plotted as a function of the median visually evoked response (in µV) for each of the 14 unique stimuli designed to stimulate the LMS (black), L-M (red), and S (blue) pathways. There is a strong correlation between visual discomfort and visually evoked response ($R^2 = 0.83$, $p = 2.2e^{-4}$).

subjects and headache free controls (Supplementary Figure 8). The second harmonic response showed a similar relationship (Supplementary Figure S9).

Discussion

Summary

Our study demonstrates that visual discomfort elicited by flickering light correlates with evoked responses in early visual cortex. This measurement

supports a generally accepted theory that until now has seen limited, direct empirical support: that visual discomfort is related to large amplitude neural responses within visual cortex (Aurora & Wilkinson, 2007). Our data also demonstrate that the relationship between cortical response and visual discomfort is independent of a particular postreceptoral channel. Our findings are consistent with prior work that has examined variation in the detectability and salience of stimulus contrast directed at the postreceptoral pathways (Switkes, 2008). While there have been reports that different colors of light evoke greater discomfort (Noseda et al., 2016), it is important to note that cone signals are only experienced by the central nervous system through the coding of the retinal ganglion cells and postreceptoral channels. We can say that visual discomfort from flicker is not the domain of any particular "color" or chromatic contrast for the examined stimulus regime. This finding suggests that the relationship between cortical activity and discomfort is not limited to a particular postreceptoral channel but rather reflects a more general phenomenon of the visual system.

Comparison with prior studies

While several studies have examined the effect of stimulus variation upon visual cortex neural response or upon reports of visual discomfort, only a few studies have combined these measurements. O'Hare and colleagues (2015) reported a positive correlation between the visual discomfort evoked by static "Op art" images and VEP response across a range of spatial frequencies. Haigh et al. (2013, 2019) demonstrated that parametric variation in the color separation of isoluminant gratings was related to greater reported discomfort, greater visual cortex hemodynamic responses (as measured by near-infrared spectroscopy), and greater cortical response as measured by VEP. Our study extends this prior work by examining the specific contribution of the postreceptoral pathways to visual discomfort across temporal flicker frequency.

Prior studies that have measured ssVEP in response to flickering stimuli have found a weak (O'Hare, 2017) or negative (Bjørk, Hagen, Stovner, & Sand, 2011) correlation between visual discomfort and visual cortical response. Bjørk et al. (2011) reported a negative correlation of visual discomfort and the cortical response evoked by flickering stimuli, finding larger cortical responses for slower temporal frequencies. An important difference between our study and the work of Bjørk et al. is that we separated the induced, periodic signal component from the aperiodic component (Haller et al., 2018). Beyond reducing noise, accounting for the aperiodic signal prevents low temporal frequency stimuli from appearing as if they induce larger cortical responses.

We studied MwA and HAf subjects. Although MwA subjects had slightly (but significantly) higher visual discomfort ratings across all stimuli, we did not find a significant difference in ssVEP response between the groups. Given our small number of subjects, our study was powered only to detect large differences between the groups. Therefore, our results do not contradict the numerous prior findings of larger evoked cortical responses in migraineurs as compared to controls, although it does place constraints on the possible magnitude of any differences that may exist in the stimulus regime tested.

Narrowband gamma oscillations

Narrowband gamma oscillations have been postulated as a neural correlate for visual discomfort. These resonant neural signals between 30 and 80 Hz (Buzsáki & Wang, 2012) are evoked by a restricted set of high-contrast stimuli (Dora Hermes, Miller, Wandell, & Winawer, 2015; Hermes, Miller, Wandell, & Winawer, 2015) and do not show strong correlation with multiunit neuronal activity (Ray, Crone, Niebur, Franaszczuk, & Hsiao, 2008; Ray & Maunsell, 2011; Winawer et al., 2013). The visual features that evoke narrowband gamma are also those that tend to cause discomfort (Adjamian et al., 2004; Hermes et al., 2015; Hermes, Trenite, & Winawer, 2017). Narrowband gamma oscillations are enhanced in migraine (Coppola et al., 2007) suggesting they represent network dynamics involved in hypersensitivity to visual stimuli. While these signals can be measured in surface EEG data (Long, Burke, & Kahana, 2014), we did not find in our data evidence that our stimuli evoke narrowband gamma (Supplementary Figure S10).

Pain pathways involved in photophobia

Our data do not assign a causal relationship between cortical activity and the sensation of discomfort. Multiple neural pathways have been implicated in visual discomfort, only some of which involve the visual cortex (for review, see Digre & Brennan, 2012). Projections of melanopsin-containing intrinsically photosensitive retinal ganglion cells (ipRGCs) to the thalamus have been offered as a mechanism of light-induced discomfort that does not involve the visual cortex (Noseda et al., 2010). However, this mechanism seems ill-suited to explain discomfort from flicker, as the stimulus variation is quite rapid relative to the slow kinetics of the ipRGCs (Do et al., 2009).

An "out-of-gamut" error

The widely accepted theory of "visual stress" posits that the experience of visual discomfort corresponds to overactivation of the visual cortex (Wilkins, 1995). Our work supports this idea and further demonstrates that the relationship between cortical response and visual discomfort is general, operating across the three postreceptoral visual pathways. While consistent with the empirical data, it is less clear why larger amplitude visual cortex responses are aversive. "Metabolic stress" has been proposed as an explanation (Hibbard & O'Hare, 2015), although we are unaware of any evidence that stimuli such as ours are actually physically injurious to the nervous system or produce demands with which the neurometabolic or neurovascular system cannot cope. We believe that, instead of viewing neural activity as a *physical* stressor upon the central nervous system, a better way of understanding visual discomfort is as a signal regarding information processing.

It is our view that visual discomfort is just what it feels like to be a neural system in an inefficient signal processing range. This "out-of-gamut" account of visual discomfort does away with the need to identify a putative physical injury or metabolic limit caused by visual stimulation. Comparison might be made to the unpleasant sensation that accompanies the receipt of mismatched visual and vestibular signals. The error signal may itself be the aversive experience.

This view is consistent with a growing body of literature that has found that stimuli are perceived as unpleasant when their spatial and temporal content departs from the statistics of natural environments (Juricevic et al., 2010; Penacchio & Wilkins, 2015; Yoshimoto et al., 2017). The visual system is remarkably adaptive across long and short time scales, and an important function of that adaptation is to allow neurons to encode sensory information using a range of representation that is well matched to the current statistics of the environment (Barlow, 2001). Our stimuli were distinctly unnatural (widefield, high contrast, sinusoidal flicker) and thus well suited to place neural coding at a representational disadvantage.

Conclusions

We find a linear relationship between visual discomfort and visual cortex response, providing empirical support to the long-standing theory of visual stress. Visual discomfort from temporal flicker is not the unique domain of a particular chromatic or achromatic postreceptoral pathway.

Acknowledgments

References

Adjamian, P., Holliday, I. E., Barnes, G. R., Hillebrand, A., Hadjipapas, A., & Singh, K. D. (2004). Induced visual illusions and gamma oscillations in human primary visual cortex. *European Journal of Neuroscience, 20*(2), 587–592, https://doi.org/10.1111/j.1460-9568.2004.03495.x.

Aurora, S. K., & Wilkinson, F. (2007). The brain is hyperexcitable in migraine. *Cephalalgia, 27*(12), 1442–1453, https://doi.org/10.1111/j.1468-2982.2007.01502.x.

Barlow, H. (2001). The exploitation of regularities in the environment by the brain. *Behavioral and Brain Sciences, 24*(4), 602–607, https://doi.org/10.1017/S0140525X01000024.

Bjørk, M., Hagen, K., Stovner, L. J., & Sand, T. (2011). Photic EEG-driving responses related to ictal phases and trigger sensitivity in migraine: A longitudinal, controlled study. *Cephalalgia, 31*(4), 444–455, https://doi.org/10.1177/0333102410385582.

Buzsáki, G., & Wang, X.-J. (2012). Mechanisms of gamma oscillations. *Annual Review of Neuroscience, 35*, 203–225, https://doi.org/10.1146/annurev-neuro-062111-150444.

Choi, J. Y., Oh, K., Kim, B. J., Chung, C. S., Koh, S. B., & Park, K. W. (2009). Usefulness of a photophobia questionnaire in patients with migraine. *Cephalalgia, 29*, 953–959, https://doi.org/10.1111/j.1468-2982.2008.01822.x.

Clark, J. H. (1924). The Ishihara test for color blindness. *American Journal of Physiological Optics, 5*, 269–276.

Comission Internationale de L'Eclairage (CIE). (2005). *Fundamental chromaticity diagram with*

physiological axes: Part 1 (CIE 16x:2005). Commission Internationale De L'Eclairage CIE Central Bureau: Vienna, Austria

Conlon, E. G., Lovegrove, W. J., Chekaluk, E., & Pattison, P. E. (1999). Measuring visual discomfort. *Visual Cognition, 6*(6), 637–663, https://doi.org/10.1080/135062899394885.

Coppola, G., Ambrosini, A., Di Clemente, L., Magis, D., Fumal, A., Geŕard, P., . . . Schoenen, J. (2007). Interictal abnormalities of gamma band activity in visual evoked responses in migraine: An indication of thalamocortical dysrhythmia? *Cephalalgia, 27*(12), 1360–1367, https://doi.org/10.1111/j.1468-2982.2007.01466.x.

Datta, R., Aguirre, G. K., Hu, S., Detre, J. A., & Cucchiara, B. (2013). Interictal cortical hyperresponsiveness in migraine is directly related to the presence of aura. *Cephalalgia, 33*, 365–374, https://doi.org/10.1177/0333102412474503.

Di Russo, F., Pitzalis, S., Aprile, T., Spitoni, G., Patria, F., Stella, A., . . . Hillyard, S. A. (2007). Spatiotemporal analysis of the cortical sources of the steady-state visual evoked potential. *Human Brain Mapping, 28*(4), 323–334, https://doi.org/10.1002/hbm.20276.

Digre, K. B., & Brennan, K. C. (2012). Shedding light on photophobia. *Journal of Neuro-Ophthalmology, 32*(1), 68–81, https://doi.org/10.1097/WNO.0b013e3182474548.

Do, M. T. H., Kang, S. H., Xue, T., Zhong, H., Liao, H. W., Bergles, D. E., . . . Yau, K. W. (2009). Photon capture and signalling by melanopsin retinal ganglion cells. *Nature, 457*, 281–287, https://doi.org/10.1038/nature07682.

Estev́ez, O., & Spekreijse, H. (1982). The "silent substitution" method in visual research. *Vision Research, 22*(6), 681–691, https://doi.org/10.1016/0042-6989(82)90104-3.

Fernandez, D., & Wilkins, A. J. (2008). Uncomfortable images in art and nature. *Perception, 37*(7), 1098–1113, https://doi.org/10.1068/p5814.

Goadsby, P., Lipton, R., & Ferrari, M. (2002). Migraine: Current understanding and treatment. *New England Journal of Medicine, 346*, 257–270, https://doi.org/10.1056/NEJMra010917.

Haigh, S. M., Barningham, L., Berntsen, M., Coutts, L. V., Hobbs, E. S. T., Irabor, J., . . . Wilkins, A. J. (2013). Discomfort and the cortical haemodynamic response to coloured gratings. *Vision Research, 89*, 47–53, https://doi.org/10.1016/j.visres.2013.07.003.

Haigh, S. M., Chamanzar, A., Grover, P., & Behrmann, M. (2019). Cortical hyper-excitability in migraine in response to chromatic patterns. *Headache, 59*, 1773–1787, https://doi.org/10.1111/head.13620.

Haller, M., Donoghue, T., Peterson, E. J., Varma, P., Sebastian, P., Gao, R., . . . Voytek, B. (2018). Parameterizing neural power spectra. *BioRxiv*, https://doi.org/10.1101/299859.

Hawken, M. J., Shapley, R. M., & Grosof, D. H. (1996). Temporal-frequency selectivity in monkey visual cortex. *Visual Neuroscience, 13*(3), 477–492, https://doi.org/10.1017/s0952523800008154.

Hermes, D., Miller, K. J., Wandell, B. A., & Winawer, J. (2015). Stimulus dependence of gamma oscillations in human visual cortex. *Cerebral Cortex, 25*(9), 2951–2959, https://doi.org/10.1093/cercor/bhu091.

Hermes, Dora, Kasteleijn-Nolst Trenite, D. G. A., & Winawer, J. (2017). Gamma oscillations and photosensitive epilepsy. *Current Biology, 27*(9), PR336–R338, https://doi.org/10.1016/j.cub.2017.03.076.

Hermes, Dora, Miller, K. J., Wandell, B. A., & Winawer, J. (2015, 2). Gamma oscillations in visual cortex: the stimulus matters. *Trends in Cognitive Sciences, 19*(2), P57–58, https://doi.org/10.1016/j.tics.2014.12.009.

Hibbard, P. B., & O'Hare, L. (2015). Uncomfortable images produce non-sparse responses in a model of primary visual cortex. *Royal Society Open Science, 2*(2), 2054–5703, https://doi.org/10.1098/rsos.140535.

Huang, J., Cooper, T. G., Satana, B., Kaufman, D. I., & Cao, Y. (2003). Visual distortion provoked by a stimulus in migraine associated with hyperneuronal activity. *Headache, 43*(6), 664–671, https://doi.org/10.1046/j.1526-4610.2003.03110.x.

Juricevic, I., Land, L., Wilkins, A., & Webster, M. A. (2010). Visual discomfort and natural image statistics. *Perception, 39*(7), 884–899, https://doi.org/10.1068/p6656.

Kaiser, E., Igdalova, A., Aguirre, G., & Cucchiara, B. (2019). A web-based, branching logic questionnaire for the automated classification of migraine. *BioRxiv. Cephalalgia, 39*(10), 1257–1266, https://doi.org/10.1177/0333102419847749.

Kelly, D. H. (1974). Spatio-temporal frequency characteristics of color—vision mechanisms. *Journal of the Optical Society of America, 64*(7), 983–990, https://doi.org/10.1364/JOSA.64.000983.

Long, N. M., Burke, J. F., & Kahana, M. J. (2014). Subsequent memory effect in intracranial and scalp EEG. *NeuroImage, 84*, 488–494, https://doi.org/10.1016/j.neuroimage.2013.08.052.

Magnussen, S., Spillmann, L., Stürzel, F., & Werner, J.S. (2001). Filling-in of the

foveal blue scotoma. Vision Research, https://doi.org/10.1016/S0042-6989(01)00178-X.

Noseda, R, Reuven-Nir, R., Bernstein, C., Borsook, D., Buettner, C., & Burstein, R. (2017). Green light alleviates migraine photophobia. *Neurology, 88*(16 Supplement), S47.005.

Noseda, Rodrigo, Bernstein, C. A., Nir, R. R., Lee, A. J., Fulton, A. B., Bertisch, S. M., . . . Burstein, R. (2016). Migraine photophobia originating in cone-driven retinal pathways. *Brain, 139*(7), 1971–1986, https://doi.org/10.1093/brain/aww119.

Noseda, Rodrigo, Kainz, V., Jakubowski, M., Gooley, J. J., Saper, C. B., Digre, K., . . . Burstein, R. (2010). A neural mechanism for exacerbation of headache by light. *Nature Neuroscience, 13*, 239–245, https://doi.org/10.1038/nn.2475.

O'Hare, L. (2017). Steady-state VEP responses to uncomfortable stimuli. *European Journal of Neuroscience, 45*(3), 410–422, https://doi.org/10.1111/ejn.13479.

O'Hare, L., Clarke, A. D. F., Pollux, P. M. J., & Martinez-Conde, S. (2015). VEP responses to op-art stimuli. *PLoS ONE, 10*(9), e0139400, https://doi.org/10.1371/journal.pone.0139400.

Penacchio, O., & Wilkins, A. J. (2015). Visual discomfort and the spatial distribution of Fourier energy. *Vision Research, 108*, 1–7, https://doi.org/10.1016/j.visres.2014.12.013.

Ray, S., Crone, N. E., Niebur, E., Franaszczuk, P. J., & Hsiao, S. S. (2008). Neural correlates of high-gamma oscillations (60–200 Hz) in macaque local field potentials and their potential implications in electrocorticography. *Journal of Neuroscience, 28*(45), 11526–11536, https://doi.org/10.1523/jneurosci.2848-08.2008.

Ray, Supratim, & Maunsell, J. H. R. (2011). Different origins of gamma rhythm and high-gamma activity in macaque visual cortex. *PLoS Biology, 9*, e1000610, https://doi.org/10.1371/journal.pbio.1000610.

Regan, D. (1983). Spatial frequency mechanisms in human vision investigated by evoked potential recording. *Vision Research, 23*(12), 1401–1407, https://doi.org/10.1016/0042-6989(83)90151-7.

Robson, J. G. (1966). Spatial and temporal contrast-sensitivity functions of the visual system. *Journal of the Optical Society of America, 56*(8), 1141–1142, https://doi.org/10.1364/josa.56.001141.

Shibata, K., Yamane, K., Nishimura, Y., Kondo, H., & Otuka, K. (2011). Spatial frequency differentially affects habituation in migraineurs: A steady-state visual-evoked potential study. *Documenta Ophthalmologica, 123*, 65, https://doi.org/10.1007/s10633-011-9281-2.

Spitschan, M., Aguirre, G. K., & Brainard, D. H. (2015). Selective stimulation of penumbral cones reveals perception in the shadow of retinal blood vessels. *PLoS ONE, 10*(4), e0124328, https://doi.org/10.1371/journal.pone.0124328.

Spitschan, M., Datta, R., Stern, A. M., Brainard, D. H., & Aguirre, G. K. (2016). Human visual cortex responses to rapid cone and melanopsin-directed flicker. *Journal of Neuroscience, 36*(5), 1471–1482, https://doi.org/10.1523/JNEUROSCI.1932-15.2016.

Switkes, E. (2008). Contrast salience across three-dimensional chromoluminance space. *Vision Research, 48*(17), 1812–1819, https://doi.org/10.1016/j.visres.2008.05.014.

Taveras Cruz, Y., He, J., & Eskew, R.T. (September 2019). *Using S-Cone signals to detect the effects of longitudinal chromatic aberration.* Paper presented at the OSA Fall Vision Meeting, Washington, DC.

Tyler, C. W., Apkarian, P., Levi, D. M., & Nakayama, K. (1979). Rapid assessment of visual function: An electronic sweep technique for the pattern visual evoked potential. *Investigative Ophthalmology and Visual Science, 18*, 703–713.

Wilkins, A. J. (1995). *Visual stress.* New York, NY: Oxford University Press.

Winawer, J., Kay, K. N., Foster, B. L., Rauschecker, A. M., Parvizi, J., & Wandell, B. A. (2013). Asynchronous broadband signals are the principal source of the bold response in human visual cortex. *Current Biology, 23*(13), 1145–1153, https://doi.org/10.1016/j.cub.2013.05.001.

Yoshimoto, S., Garcia, J., Jiang, F., Wilkins, A. J., Takeuchi, T., & Webster, M. A. (2017). Visual discomfort and flicker. *Vision Research, 138*, 18–28, https://doi.org/10.1016/j.visres.2017.05.015.